# Appendix: Supporting Information

# Dynamics of Trophoblast Differentiation in Peri-implantation Stage Human Embryos

**Authors:** Rachel C. West[1†], Hao Ming[2†], Deirdre M. Logsdon[1†], Jiangwen Sun[3], Sandeep K. Rajput[1], Rebecca A. Kile[1], William B. Schoolcraft[1], R. Michael Roberts[4]*, Rebecca L. Krisher[1], Zongliang Jiang[2]*, Ye Yuan[1]*

## Materials and Methods

**Western blotting.** Western blot analysis was used to determine the expression and phosphorylation level of target proteins. Embryos were manually removed from culture plates and washed in 0.01% polyvinyl alcohol (PVA) in PBS. Embryos were lysed in 20 μL of RIPA buffer (Sigma; #R0278) containing a phosphatase inhibitor and protease inhibitor cocktail. Lysate was mixed with 4X Laemmli buffer and incubated for 5 min at room temperature (RT) before boiling at 100˚C for 10 min. Samples were cooled to RT and then analyzed on 4-20% Mini-Protean TGX Precast gels (Bio-Rad, #4561093) at 150V for 70 min. After running, protein-SDS complexes were transferred onto a PVDF membrane (Millipore; #IPVH00010) at 95V for 65 min. The membrane was then incubated in blocking buffer (3 % w/v BSA in 1X TBST) at room temperature for 1 h and probed with primary antibodies (Table S5) at a 1:5000 dilution in blocking buffer at 4˚C overnight. Membranes were washed 3-4 times for 3 min in 1X TBST and incubated with corresponding secondary antibody (also at a 1:5000 dilution in blocking buffer) at RT for 1 h. Membranes were again washed 3 times in 1 X TBST then incubated in SuperSignal West Dura Chemiluminescent substrate (Thermo Scientific; #34076) for 2 min. Protein band images were captured by using ChemiDoc XRS (Bio-Rad Laboratories). Quantitative densitometry analysis was performed with ImageJ software (http://imagej.nih.gov/ij/) and expression normalized relative to actin (ACTB). The ratio of phosphorylated and total protein abundance was used to determine the phosphorylation level of target proteins.



www.pnas.org/cgi/doi/10.1073/pnas.1911362116

**Enzyme-Linked Immunosorbent Assay (ELISA).** Medium was collected at D8, D10, and D12 and frozen at -80°C until assays (n = 5). iIFNA was measured with an Affymetrix eBiosciences ELISA kit (ThermoFisher Scientific, BMS216) according to manufacturer's directions with an Epoch Microplate spectrophotometer (BioTek) used to measure absorbance.

**Endotoxin Assay.** To determine if embryo culture medium had been contaminated by exogenous endotoxins, a Limulus ameobocyte lysate (LAL) assay was performed with the Endosafe Cartridge system (Charles River). Randomly selected samples of medium from 9 different time points were analyzed. All samples had the same (undetectable) endotoxin levels as fresh IVC1 and IVC2 medium (Table S6).

**Electrochemiluminescence Assay (ECLIA).** Human hCG in the embryo culture medium was measured daily with the Elecsys HCG STAT kit (Roche Diagnostics), beginning at 24 h post-attachment (embryo D7) until embryo D12. Samples (n = 13) were immediately frozen and stored at -80°C. After thawing, 10 µL aliquots were added to a biotinylated hCG antibody and another monocolonal hCG-specific antibody labeled with a ruthenium complex to create a sandwich complex. After incubating, streptavidin-coated microparticles were added to the mixture. The mixture was added to the measuring cell of the Cobas system, and results calculated. Raw results were normalized and, to account for daily medium changes, raw values were multiplied by 2. Then the previous day's measured concentration was subtracted from the value, i.e. D9 actual concentration = (D9 measure concentration x 2) – D8 concentration.

**Statistical Analysis.** Statistical analysis was performed with One-Way ANOVA followed by Tukey's test with the Prism8 Software (Graphpad). P-values less than 0.05 were considered likely to represent a significant difference between entities.

**Figure S1. Expression of epiblast marker POU5F1, TB markers KRT7 and GATA3 in human D10 embryos. (A)** A 3D montage of a D10 human embryo demonstrating the multi-nucleated syncytium located on the periphery (indicated by arrows), and POU5F1 positive epiblast cells confined to the central area of the embryo. **(B)** POU5F1 positive epiblast cells formed the embryonic disc (Left panel) (experiment performed on three separate embryos); Expression of KRT7 and GATA3 in human D10 embryos (Middle and right panel, respectively) (experiment performed on three separate embryos).

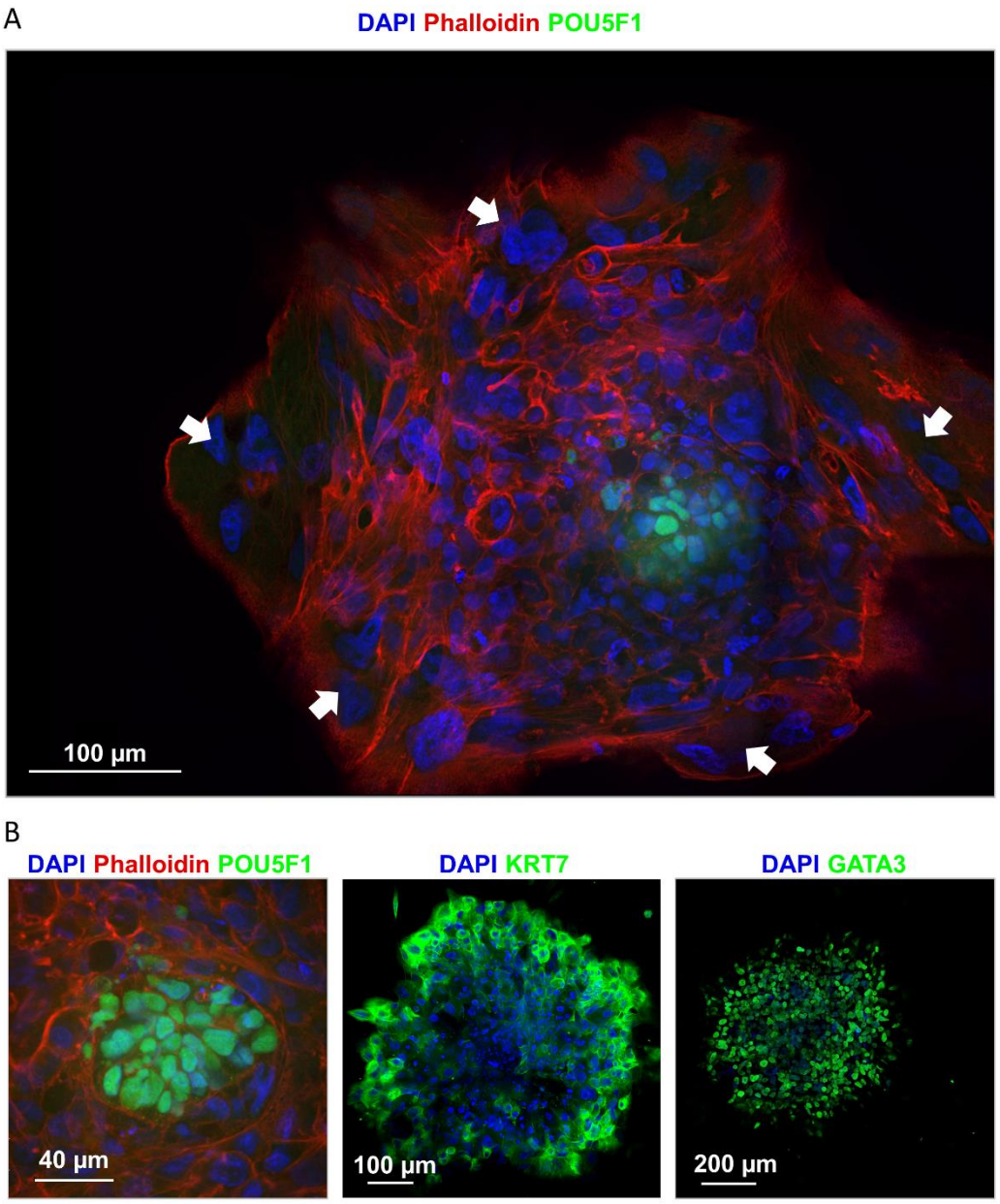

**Figure S2. Filtration of sequencing data.** (**A**) 14,105 genes had maximum FPKM values of at least 1, and 15,420 genes had FPKM values of at least 0.3 in at least 4 cells. Genes with FPKM values of less than 0.3 in at least 4 cells were removed from analysis. (**B**) CTB cells expressed more genes than STB and MTB cells. However, there was no significant increase in number of expressed genes between D8, D10, and D12.

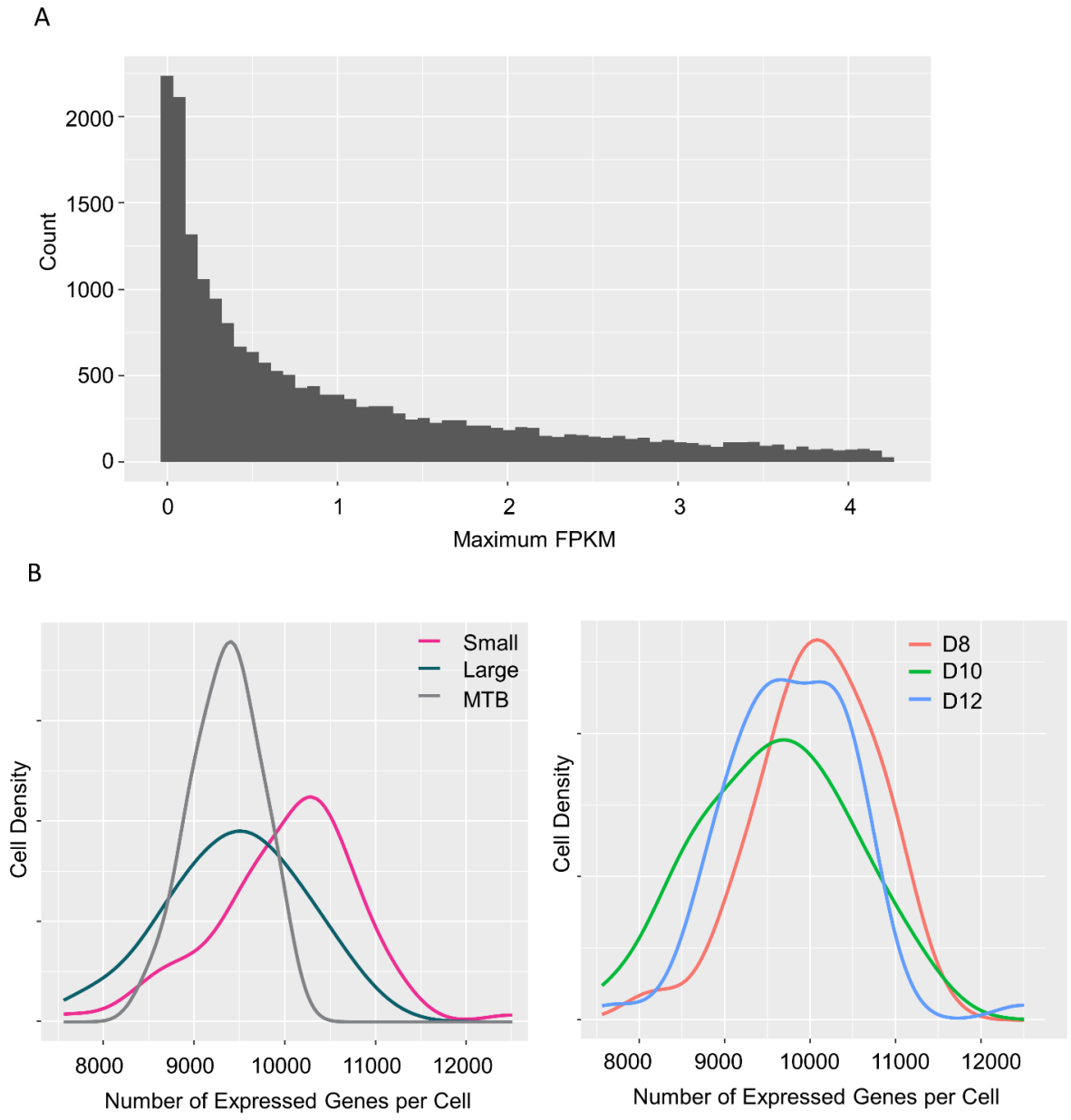

**Figure S3.** Principal component analysis of TB cells clustered by cell type (A) or developmental stage (B).

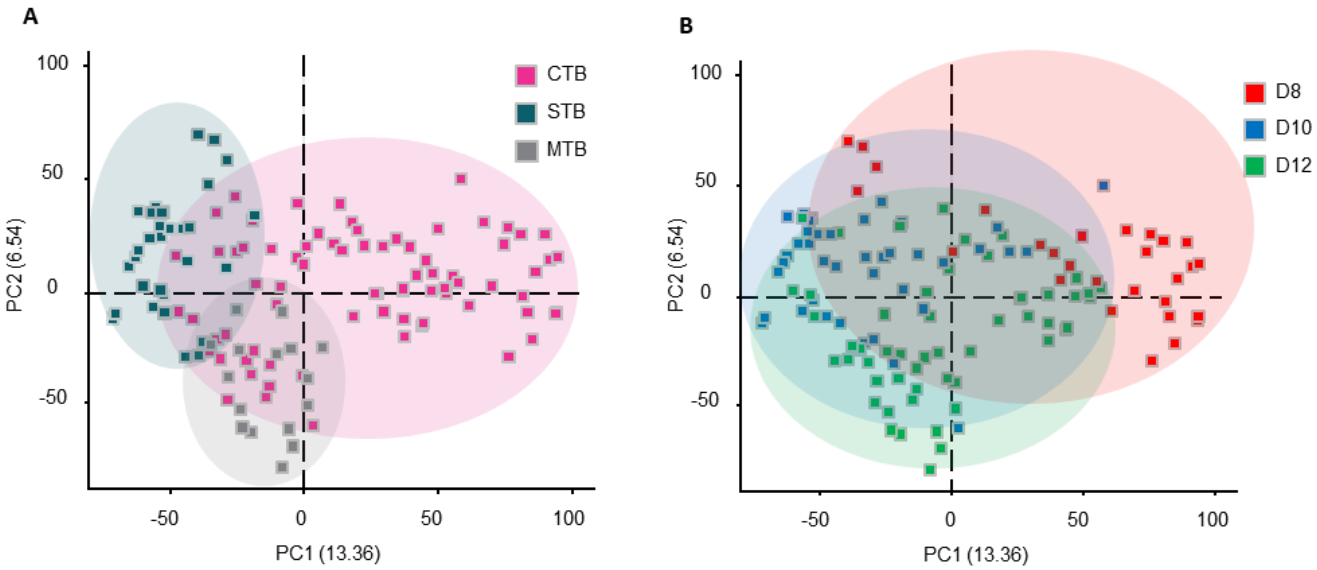

**Figure S4. Gene ontology and pathway analysis of cell type specific genes for CTB, STB, and MTB.** Top GO terms and pathways for CTB involved cell division, RNA processing and transport, and energy metabolism. GO terms and pathways for STB involved protein folding, transport, and hormone production. GO terms and pathways for MTB revealed upregulation of genes necessary of cell migration, invasion, vasculature remodeling, and immune response.

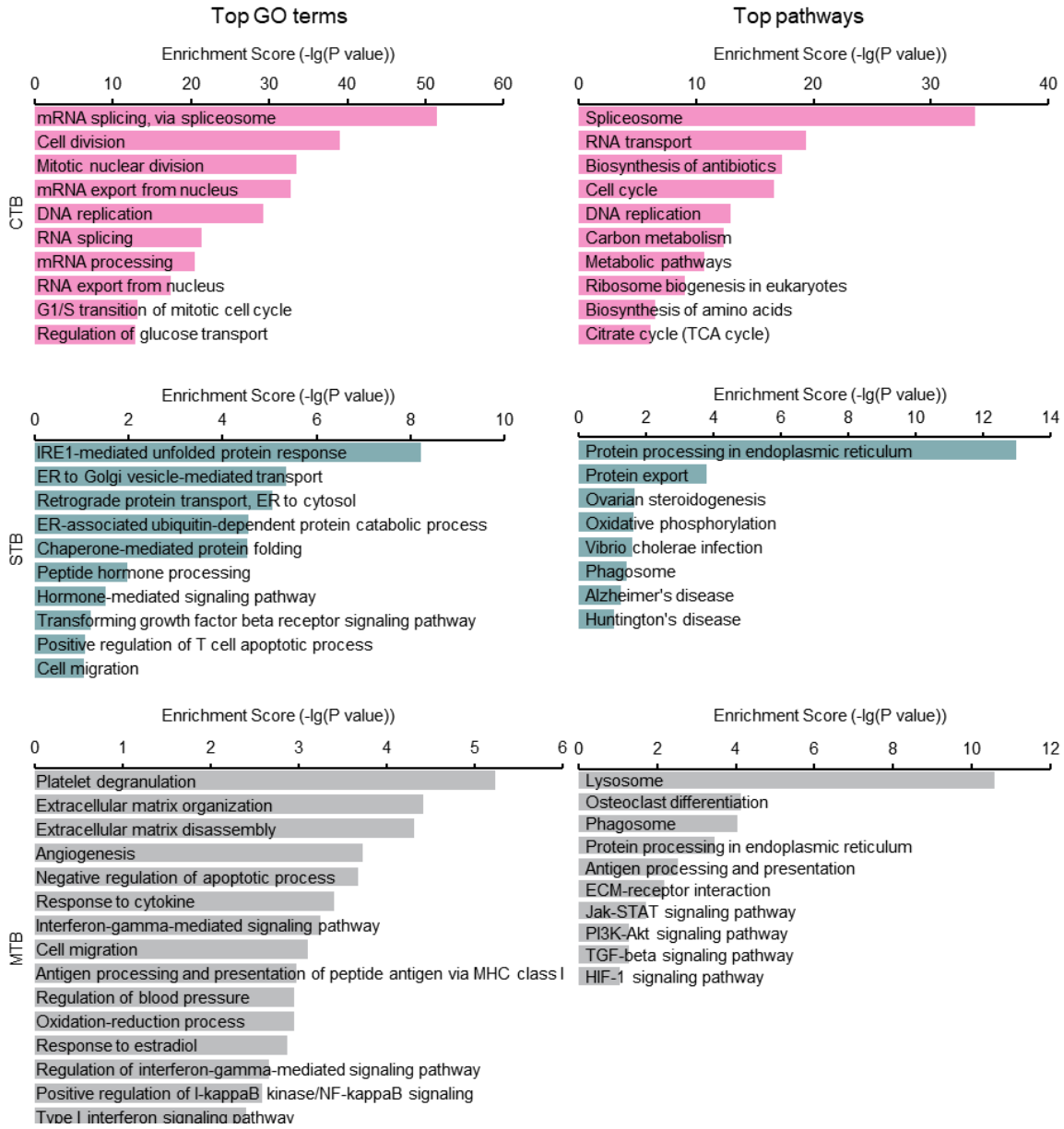

**Figure S5. Gene ontology and pathway analysis of D8, D10, and D12 CTB.** Top GO terms and pathways for D8 CTB include cell proliferation, transcription, and energy metabolism, whereas by D10, the focus had shifted to hormone production, syncytialization, and protein processing. At D12, top pathways have further shifted towards angiogenesis, hypoxia, and interferon signaling.

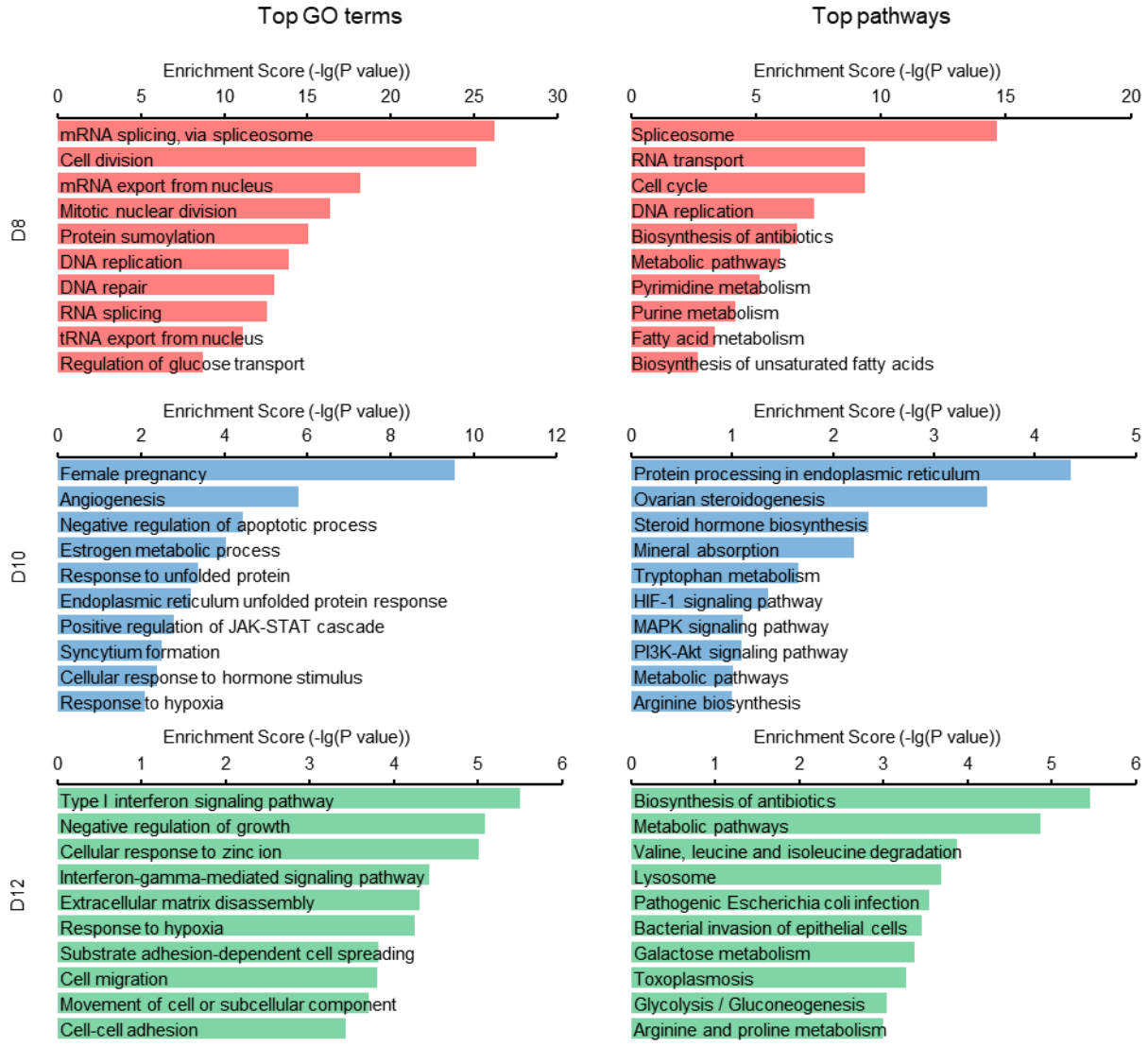

**Fig. S6. Comparing GO terms and pathway analysis between (A) CTB, pre-STB, and STB and (B) CTB, pre-MTB, and MTB.** The GO terms and pathway analysis of pre-STB cells showed a mix of CTB and STB processes. Pre-STB cells still have evidence for mitosis while also demonstrating GO terms important for STB function such as syncytium formation, cell differentiation, and protein processing. An analogous phenomenon also holds true for pre-MTB cells, since these cells have pathways linked to proliferation as well as migration and invasion, immunomodulation etc.

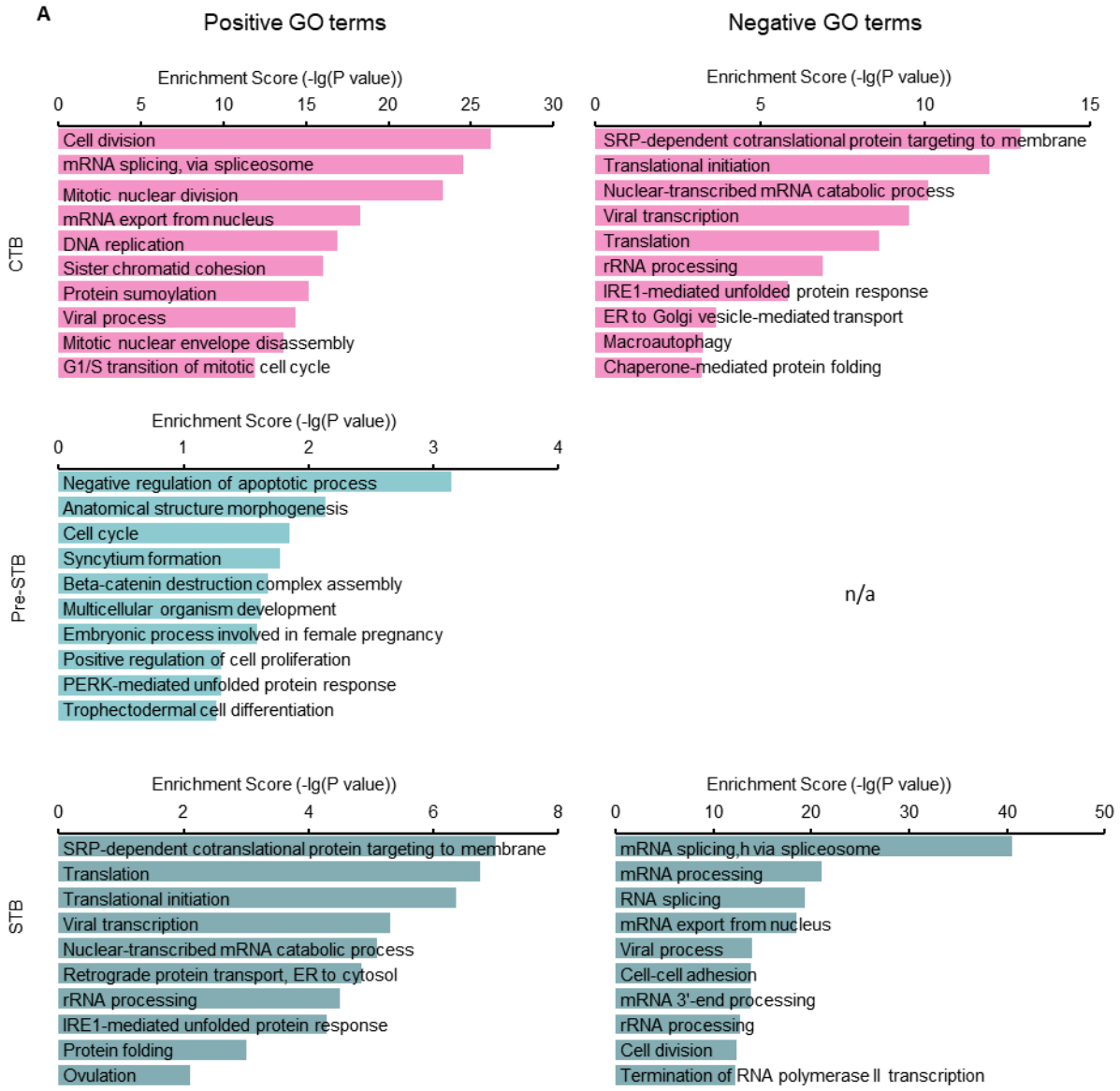

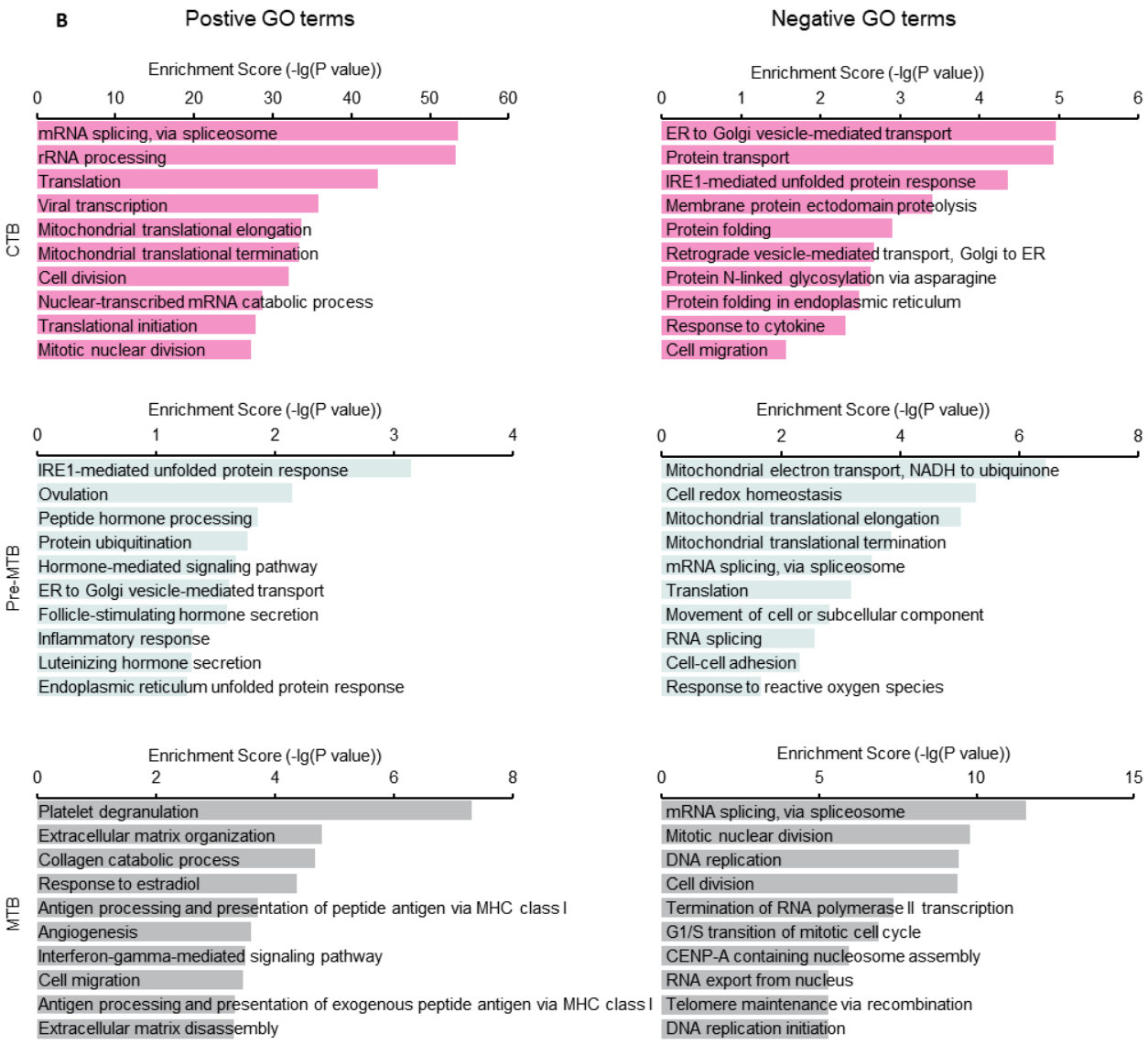
B
Postive GO terms
Negative GO terms
Enrichment Score (-lg(P value))
CTB
mRNA splicing, via spliceosome
rRNA processing
Translation
Viral transcription
Mitochondrial translational elongation
Mitochondrial translational termination
Cell division
Nuclear-transcribed mRNA catabolic process
Translational initiation
Mitotic nuclear division
ER to Golgi vesicle-mediated transport
Protein transport
IRE1-mediated unfolded protein response
Membrane protein ectodomain proteolysis
Protein folding
Retrograde vesicle-mediated transport, Golgi to ER
Protein N-linked glycosylation via asparagine
Protein folding in endoplasmic reticulum
Response to cytokine
Cell migration
Pre-MTB
IRE1-mediated unfolded protein response
Ovulation
Peptide hormone processing
Protein ubiquitination
Hormone-mediated signaling pathway
ER to Golgi vesicle-mediated transport
Follicle-stimulating hormone secretion
Inflammatory response
Luteinizing hormone secretion
Endoplasmic reticulum unfolded protein response
Mitochondrial electron transport, NADH to ubiquinone
Cell redox homeostasis
Mitochondrial translational elongation
Mitochondrial translational termination
mRNA splicing, via spliceosome
Translation
Movement of cell or subcellular component
RNA splicing
Cell-cell adhesion
Response to reactive oxygen species
MTB
Platelet degranulation
Extracellular matrix organization
Collagen catabolic process
Response to estradiol
Antigen processing and presentation of peptide antigen via MHC class I
Angiogenesis
Interferon-gamma-mediated signaling pathway
Cell migration
Antigen processing and presentation of exogenous peptide antigen via MHC class I
Extracellular matrix disassembly
mRNA splicing, via spliceosome
Mitotic nuclear division
DNA replication
Cell division
Termination of RNA polymerase II transcription
G1/S transition of mitotic cell cycle
CENP-A containing nucleosome assembly
RNA export from nucleus
Telomere maintenance via recombination
DNA replication initiation

**Figure S7.** FPKM values of the cell proliferation marker *PCNA* and *MCM* genes in different sub-types of early TB cells.

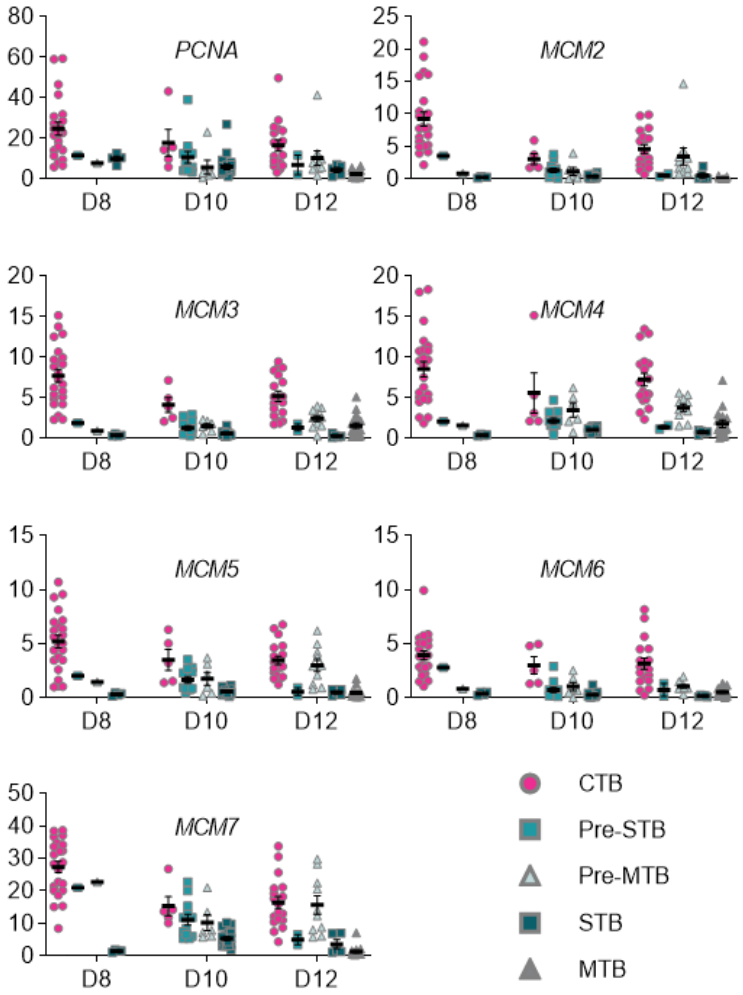

**Figure S8.** **(A)** FPKM values of MHC class I genes (*HLA-C*, *HLA-E* and *HLA-G*) in human embryos between D8 and D12. **(B)** Immunofluorescence of HLA-G in D12 human embryos (n=3). HLA-G is exclusively expressed in cells located on the periphery of the D12 embryo. (**C**) FPKM values of MHC class II genes (*HLA-DOB* and *HLA-DRB1*) in human embryos between D8 and D12.

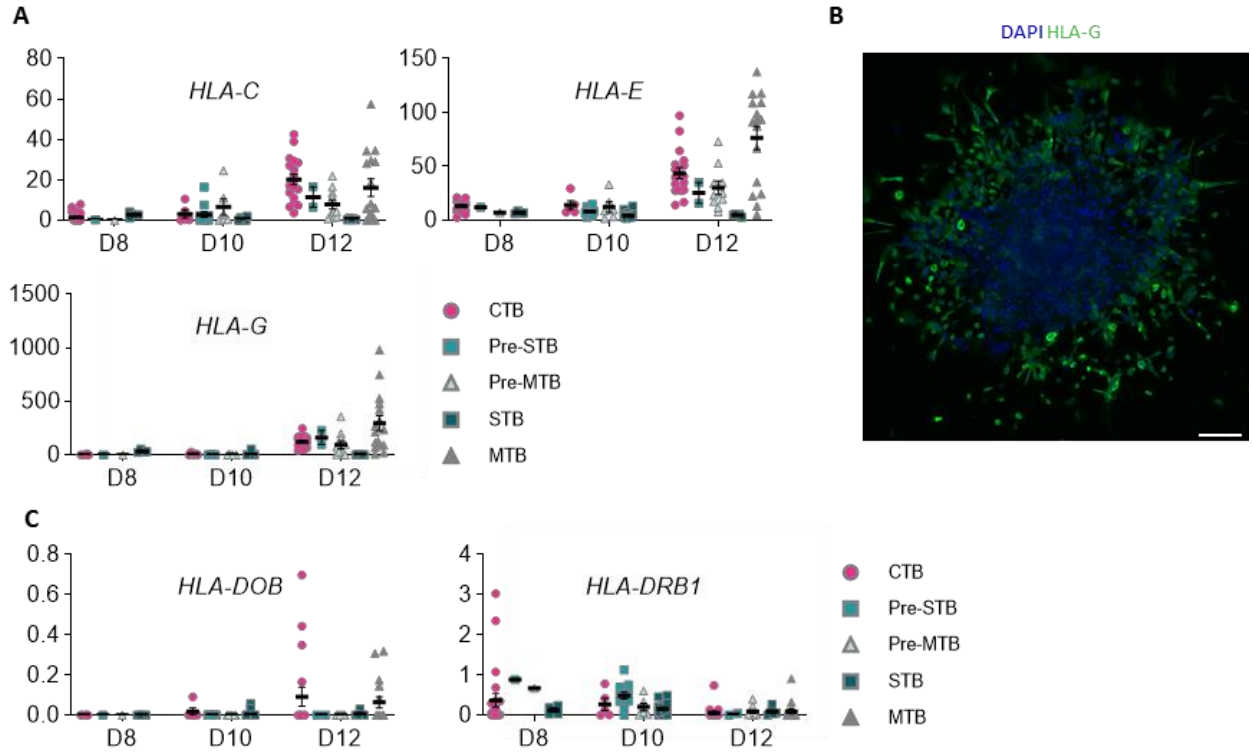

**Table S1.** Embryo donor age, body mass index (BMI), embryo grade and infertility diagnosis*

| | Age | BMI | Embryo Grade | Diagnosis |
|---|---|---|---|---|
| **D8 E1** | 35 | 23.33 | 4AB | Unexplained infertility |
| **D8 E2** | 32 | 18.2 | 3BB | Unexplained infertility |
| **D8 E3** | 37 | 23.81 | 4AB | Secondary infertility-history of ectopic pregnancy |
| **D8 E4** | 32 | 18.2 | 3BA | Unexplained infertility |
| **D10 E1** | 35 | 20.59 | 3BB | Recurrent pregnancy loss - history of ectopic pregnancy |
| **D10 E2** | 34 | 18.91 | 4AB | Habitual abortion |
| **D10 E3** | 32 | 18.2 | 5AB | Unexplained infertility |
| **D10 E4** | 41 | 19.76 | 4AA | Infertility-AMA & history of endometriosis |
| **D12 E3** | 40 | 22.22 | 4BB | Advanced maternal age |
| **D12 E4** | 36 | 27.89 | 3BB | Recurrent pregnancy loss |
| **D12 E6** | 36 | 28.54 | 4AB | Advanced maternal age |

All embryos were donated at the conclusion of completed fertility treatment with patients' informed consent**.**

**Table S2.** Cell sample information

| | CTB | STB | MTB |
|---|---|---|---|
| **D8 E1** | 8 | 0 | 0 |
| **D8 E2** | 8 | 0 | 0 |
| **D8 E3** | 8 | 4 | 0 |
| **D8 E4** | 3 | 0 | 0 |
| **D10 E1** | 8 | 3 | 0 |
| **D10 E2** | 8 | 11 | 0 |
| **D10 E3** | 8 | 0 | 0 |
| **D10 E4** | 4 | 6 | 0 |
| **D12 E3** | 24 | 0 | 4 |
| **D12 E4** | 4 | 6 | 12 |
| **D12 E6** | 4 | 6 | 0 |

**Table S3.** FPKM values of gene markers used to determine cell lineages*

| | Sample ID | | | | | | |
|---|---|---|---|---|---|---|---|
| | **D10_E3_C1** | **D12_E4_C3** | **D12_E6_S6** | **D8_E3_S1** | **D8_E4_C1** | **D8_E4_C2** | **D8_E4_C3** |
| ***POU5F1*** | 1.89 | 0.03 | 0 | 0.26 | 37.26 | 0 | 0 |
| ***GATA6*** | 0.35 | 0.04 | 0.08 | 0 | 0.28 | 0 | 0.20 |
| ***KRT7*** | 0.52 | 17.69 | 3.41 | 12.03 | 5.24 | 9.86 | 12.96 |
| ***GATA3*** | 3.40 | 3.98 | 2.16 | 1.70 | 2.86 | 23.25 | 12.00 |
| ***CDX2*** | 0 | 0 | 0 | 0 | 0 | 0 | 0 |
| ***SOX2*** | 2.39 | 0 | 0.06 | 0 | 21.03 | 0 | 0 |
| ***NANOG*** | 0.03 | 0.01 | 0.02 | 0.36 | 39.65 | 0.01 | 0.02 |
| ***CD24*** | 9.34 | 0.31 | 3.92 | 5.60 | 11.20 | 0.05 | 0.88 |

*'D10_E3_C1' and 'D8_E4_C1' were considered as epiblast cells and excluded from the analysis. The others were considered as TB and remained in the analysis. The Sample ID "D10_E3_C1" indicates CTB from D10 Embryo 3.

**Table S4.** Primary antibodies for Immunofluorescence.

| Protein | Antibody | Host | Dilution |
|---|---|---|---|
| IFNAR1 | Santa Cruz, sc-7391 | Mouse | 1:200 |
| IFNGR1 | Abcam, Ab200327 | Rabbit | 1:200 |
| ISG15 | Santa Cruz, sc-166755 | Mouse | 1:200 |
| ISG20 | Abcam, ab198801 | Rabbit | 1:200 |
| HLA-G | Santa Cruz, sc-21799 | Mouse | 1:200 |
| ERVW1 | Abcam, Ab234850 | Rabbit | 1:200 |

**Table S5.** Sources of primary antibodies for Western Blotting.

| Protein | Antibody | Host |
|---|---|---|
| STAT1 | Cell Signaling, #9172 | Rabbit |
| Phospho-STAT1 | Cell Signaling, #9177 | Rabbit |
| AKT | Cell Signaling, #4691S | Rabbit |
| Phospho-AKT | Cell Signaling, #4060S | Rabbit |
| MAPK1/3 | Cell Signaling, #4695S | Rabbit |
| Phospho-MAPK1/3 | Cell Signaling, #4370S | Rabbit |
| HRP Anti-Rabbit IgG | Thermo Scientific, #PA1-74421 | Mouse |

**Table S6.** Endotoxin levels in culture medium.

| Medium | Concentration (EU/mL) |
|---|---|
| IVC1 | 0.006 |
| IVC2 | 0.009 |
| 24h Post-Attachment | 0.005 |
| 48h Post-Attachment | 0.006 |
| 74h Post-Attachment | 0.006 |

**Movie S1.** Time-lapse imaging of an extended cultured human embryo between D8-D12. Using time-lapse imaging, extended embryo culture development was captured every 30 min between D8 and D12. Imaging reveals the collapse of the blastocoel, the formation of the primitive syncytium (indicated by the green circles), and the eventual differentiation and migration of MTB (indicated by the orange circles).

**Dataset S1.** Sources of marker genes for CTB, STB, and MTB ranked by P-value.


1. G. E. Jarvis, Early embryo mortality in natural human reproduction: What the data say. *F1000Research* **5**, 2765 (2016).
2. N. S. Macklon, J. P. Geraedts, B. C. Fauser, Conception to ongoing pregnancy: the 'black box' of early pregnancy loss. *Hum Reprod Update* **8**, 333-343 (2002).
3. A. M. Carter, Animal models of human placentation--a review. *Placenta* **28 Suppl A**, S41-47 (2007).
4. A. C. Enders, Trophoblast-uterine interactions in the first days of implantation: models for the study of implantation events in the human. *Semin Reprod Med* **18**, 255-263 (2000).
5. A. T. Hertig, J. Rock, E. C. Adams, A description of 34 human ova within the first 17 days of development. *Am J Anat* **98**, 435-493 (1956).
6. J. D. Boyd, Hamilton, W.J., *The human placenta.* (Heffer & Sons, Cambridge., 1970).
7. E. Amoroso, "Placentation." in Marshall's Physiology of Reproduction, A. Parkes, Ed. (Little Brown & Co., Boston, 1952), vol. 2, pp. 127-311.
8. A. C. Enders, Trophoblast differentiation during the transition from trophoblastic plate to lacunar stage of implantation in the rhesus monkey and human. *Am J Anat* **186**, 85-98 (1989).
9. A. C. Enders, B. F. King, Early stages of trophoblastic invasion of the maternal vascular system during implantation in the macaque and baboon. *Am J Anat* **192**, 329-346 (1991).
10. A. C. Enders, K. C. Lantz, P. E. Peterson, A. G. Hendrickx, From blastocyst to placenta: the morphology of implantation in the baboon. *Hum Reprod Update* **3**, 561-573 (1997).
11. J. Hustin, J. P. Schaaps, Echographic [corrected] and anatomic studies of the maternotrophoblastic border during the first trimester of pregnancy. *Am J Obstet Gynecol* **157**, 162-168 (1987).
12. J. M. Foidart, J. Hustin, M. Dubois, J. P. Schaaps, The human placenta becomes haemochorial at the 13th week of pregnancy. *Int J Dev Biol* **36**, 451-453 (1992).
13. G. J. Burton, E. Jauniaux, A. L. Watson, Maternal arterial connections to the placental intervillous space during the first trimester of human pregnancy: the Boyd collection revisited. *Am J Obstet Gynecol* **181**, 718-724 (1999).
14. J. L. James, A. M. Carter, L. W. Chamley, Human placentation from nidation to 5 weeks of gestation. Part I: What do we know about formative placental development following implantation? *Placenta* **33**, 327-334 (2012).
15. R. H. Xu *et al.*, BMP4 initiates human embryonic stem cell differentiation to trophoblast. *Nature biotechnology* **20**, 1261-1264 (2002).

16. S. Yabe *et al.*, Comparison of syncytiotrophoblast generated from human embryonic stem cells and from term placentas. *Proceedings of the National Academy of Sciences of the United States of America* **113**, E2598-2607 (2016).
17. H. Okae *et al.*, Derivation of Human Trophoblast Stem Cells. *Cell Stem Cell* **22**, 50-63 e56 (2018).
18. S. Haider *et al.*, Self-Renewing Trophoblast Organoids Recapitulate the Developmental Program of the Early Human Placenta. *Stem Cell Reports* **11**, 537-551 (2018).
19. M. Y. Turco *et al.*, Trophoblast organoids as a model for maternal-fetal interactions during human placentation. *Nature* **564**, 263-267 (2018).
20. A. Deglincerti *et al.*, Self-organization of the in vitro attached human embryo. *Nature* **533**, 251-254 (2016).
21. M. N. Shahbazi *et al.*, Self-organization of the human embryo in the absence of maternal tissues. *Nat Cell Biol* **18**, 700-708 (2016).
22. L. Yan *et al.*, Single-cell RNA-Seq profiling of human preimplantation embryos and embryonic stem cells. *Nat Struct Mol Biol* **20**, 1131-1139 (2013).
23. P. Blakeley *et al.*, Defining the three cell lineages of the human blastocyst by single-cell RNA-seq. *Development* **142**, 3613 (2015).
24. S. Petropoulos *et al.*, Single-Cell RNA-Seq Reveals Lineage and X Chromosome Dynamics in Human Preimplantation Embryos. *Cell* **165**, 1012-1026 (2016).
25. M. Knofler, J. Pollheimer, Human placental trophoblast invasion and differentiation: a particular focus on Wnt signaling. *Frontiers in genetics* **4**, 190 (2013).
26. B. K. Tye, MCM proteins in DNA replication. *Annual review of biochemistry* **68**, 649-686 (1999).
27. Z. Kelman, PCNA: structure, functions and interactions. *Oncogene* **14**, 629-640 (1997).
28. L. C. Platanias, Mechanisms of type-I- and type-II-interferon-mediated signalling. *Nat Rev Immunol* **5**, 375-386 (2005).
29. N. de Parseval, V. Lazar, J. F. Casella, L. Benit, T. Heidmann, Survey of human genes of retroviral origin: identification and transcriptome of the genes with coding capacity for complete envelope proteins. *Journal of virology* **77**, 10414-10422 (2003).
30. P. M. Johnson, T. W. Lyden, J. M. Mwenda, Endogenous retroviral expression in the human placenta. *American journal of reproductive immunology* **23**, 115-120 (1990).
31. N. S. Rote, S. Chakrabarti, B. P. Stetzer, The role of human endogenous retroviruses in trophoblast differentiation and placental development. *Placenta* **25**, 673-683 (2004).
32. J. Sugimoto, M. Sugimoto, H. Bernstein, Y. Jinno, D. Schust, A novel human endogenous retroviral protein inhibits cell-cell fusion. *Scientific reports* **3**, 1462 (2013).
33. A. Jain, T. Ezashi, R. M. Roberts, G. Tuteja, Deciphering transcriptional regulation in human embryonic stem cells specified towards a trophoblast fate. *Scientific reports* **7**, 17257 (2017).
34. C. La Bonnardiere *et al.*, Production of two species of interferon by Large White and Meishan pig conceptuses during the peri-attachment period. *J Reprod Fertil* **91**, 469-478 (1991).
35. K. Imakawa *et al.*, Interferon-like sequence of ovine trophoblast protein secreted by embryonic trophectoderm. *Nature* **330**, 377-379 (1987).
36. R. M. Roberts, Y. Chen, T. Ezashi, A. M. Walker, Interferons and the maternal-conceptus dialog in mammals. *Semin Cell Dev Biol* **19**, 170-177 (2008).

37. N. Inagaki *et al.*, Analysis of intra-uterine cytokine concentration and matrix-metalloproteinase activity in women with recurrent failed embryo transfer. *Human reproduction* **18**, 608-615 (2003).
38. G. A. Hardy *et al.*, Desensitization to type I interferon in HIV-1 infection correlates with markers of immune activation and disease progression. *Blood* **113**, 5497-5505 (2009).
39. R. Apps *et al.*, Human leucocyte antigen (HLA) expression of primary trophoblast cells and placental cell lines, determined using single antigen beads to characterize allotype specificities of anti-HLA antibodies. *Immunology* **127**, 26-39 (2009).
40. S. P. Murphy, J. C. Choi, R. Holtz, Regulation of major histocompatibility complex class II gene expression in trophoblast cells. *Reproductive biology and endocrinology : RB&E* **2**, 52 (2004).
41. S. G. Holtan, D. J. Creedon, P. Haluska, S. N. Markovic, Cancer and pregnancy: parallels in growth, invasion, and immune modulation and implications for cancer therapeutic agents. *Mayo Clinic proceedings* **84**, 985-1000 (2009).
42. B. Zhang *et al.*, Effect of Substrate Topography and Chemistry on Human Mesenchymal Stem Cell Markers: A Transcriptome Study. *Int J Stem Cells* **12**, 84-94 (2019).
43. M. Darnell, L. Gu, D. Mooney, RNA-seq reveals diverse effects of substrate stiffness on mesenchymal stem cells. *Biomaterials* **181**, 182-188 (2018).
44. G. Fasano *et al.*, A randomized controlled trial comparing two vitrification methods versus slow-freezing for cryopreservation of human cleavage stage embryos. *J Assist Reprod Genet* **31**, 241-247 (2014).
45. Z. Jiang *et al.*, Transcriptional profiles of bovine in vivo pre-implantation development. *Bmc Genomics* **15**, 756 (2014).